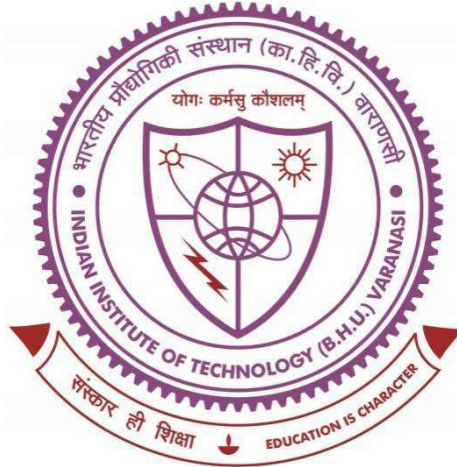


Development of Immunosensor Based on Self Assemble Monolayers  
of Polymer Metal Nanocomposites for Rapid Quantification of MSG



Thesis submitted in partial fulfilment

For the Award of Degree

**Doctor of Philosophy**

BY

**DEV DUTT SHARMA**

SCHOOL OF BIOMEDICAL ENGINEERING

INDIAN INSTITUTE OF TECHNOLOGY BHU, VARANASI, 221005, U.P.,  
INDIA

Roll No. 18021001

2022

## Certificate

It is certified that the work contained in this thesis entitled "Development of Immunosensor Based on Self Assemble Monolayers of Polymer Metal Nanocomposites for Rapid Quantification of MSG" has been carried out under my supervision, and it has not been submitted elsewhere for a degree.

It is further certified that Devdutt Sharma has fulfilled all the Comprehensive Examination, Candidacy, and SOTA requirements for the award of Ph.D. Degree.



Dr. MARSHAL  
Associate Professor  
School of Biomedical Engineering  
Indian Institute of Technology (B.H.U.)  
Varanasi-221005 (India)

**Dr. Marshal**  
(Thesis Supervisor)  
Associate Professor  
Nano-Cellular Medicine and Biophysics Laboratory  
School of Biomedical Engineering  
Indian Institute of Technology (BHU), Varanasi - 221005, UP, India.

### Declaration by the Candidate

I, Devdutt Sharma, certify that the work embodied in this thesis is my bonafide work and carried out by me from July 2018 to July 2022 under the supervision of Dr. Marshal at the Nano-Cellular Medicine and Biophysics Laboratory, School of Biomedical Engineering, India Institute of Technology (Banaras Hindu University), Varanasi 221005, UP, India.

The matter embodied in this thesis has not been submitted to award any other degree/diploma. I declare that I have faithfully acknowledged and given credits to the research worker wherever their works have been cited in this thesis. I further declare that I have not willfully copied any other's work, paragraphs, text, data, results, etc., reported in the journal, books, magazines reports, dissertations, thesis, etc., or available on websites and have not included them in this thesis and have not cited as my work.

Date : 26-07-2022  
Place : Varanasi

  
(Devdutt Sharma)

### Certificate by the Supervisor

It is certified that the above statements made by the students are correct to the best of my knowledge.



**Dr. Marshal** (Thesis Supervisor)  
Associate Professor  
Nano-Cellular Medicine and Biophysics Laboratory, School of Biomedical Engineering,  
Indian Institute of Technology (BHU), Varanasi - 221005, UP, India.

  
26.07.22  
Signature of Coordinator of the School  
समन्वयक/CO-ORDINATOR  
जैव चिकित्सा अभियांत्रिकी स्कूल  
SCHOOL OF BIOMEDICAL ENGG.  
भारतीय प्रौद्योगिकी संस्थान (का.हि.वि.)  
INDIAN INSTITUTE OF TECHNOLOGY (B.H.U.)  
वाराणसी-221005/VARANASI-221005

## **Copy Right Transfer Certificate**

**Title of the thesis:** Development of Immunosensor Based on Self-Assemble Monolayers of Polymer Metal Nanocomposites for Rapid Quantification of MSG

**Name of the student:** Devdutt Sharma

### **Copyright Transfer**

The undersigned hereby assigns to the Indian Institute of Technology (Banaras Hindu University), Varanasi – 21005, India, all right under the copyright that may exist in and for the above thesis submitted for the award of the DOCTOR OF PHILOSOPHY.

Date: 31-07-2022

Place: Varanasi

(DEV DUTT SHARMA)

**Note:** However, the author may reproduce or authorize others to reproduce material extracted verbatim from the thesis, or derivative of the thesis for the author's personal use, provided that the source and the institute's copyright notice are indicated

## ACKNOWLEDGMENT

I am thankful to my supervisor, Dr. Marshal, Associate professor, Nanocellular Medicine and Biophysics lab, School of Biomedical Engineering, India Institute of Technology (Banaras Hindu University) Varanasi 221005, UP, India, for his guidance and consistent support during my thesis.

I am grateful to him for motivating me toward achieving high research standards and enforcing strict validations for each research result, thus teaching me how to do research. I express my deep and sincere gratitude to Dr. Raju Khan, Principal Scientist, CSIR-Advanced Materials and Processes Research Institute (CSIR-AMPRI), Bhopal, India, and Dr. Hemant Sankar Dutta, Senior Scientist, Analytical Chemistry Group, CSIR-North East Institute of Science and Technology, Jorhat, India, for their consistent support in utilizing their facilities and guidance while performing experiments at their labs.

I also extend my gratitude towards my Research Progress Evaluation Committee (RPEC) members (Dr. Sanjay Singh Rai, Associate Professor, School of Biomedical Engineering, India Institute of Technology (Banaras Hindu University), Varanasi, India, and Dr. Shreyansh Kumar Jain, Assistant Professor Department of Pharmaceutical Engineering and Technology, India Institute of Technology (Banaras Hindu University), Varanasi, India) for evaluating my work and providing useful feedback to improve it on time to time. I would also like to be thankful to the office staff school of biomedical engineering, who has been supportive in every way. I would also like to be special gratitude to Mr. Barat Lal, technical supervisor, and all non-teaching staff of the school for their help and cooperation extended for the successful completion of the work. My sincere gratitude to the School of Biomedical Engineering, India Institute of Technology (Banaras Hindu University), Varanasi, which provided a platform to carry out this research work.

I am wholeheartedly thankful to my dear lab mates Rasmita Devi at Analytical Chemistry Group, CSIR-North East Institute of Science and Technology, Jorhat, India, and Juhi Jaiswal, Shenlata

Yadav, Shubangi, Shailendra Kumar and Sanju Kumari with whom I shared the lab with many ups and downs.

Few notes of gratefulness to my grandparents, Lt. Dada Ji Shri Karta Ram, and my Lt. Dadi Smt. Vidyavati Devi, my parents, Shri Radhey Shyam and Santosh Devi, and elder Sisters Tripta Sharma, Kumkum Sharma, Rajni Sharma, and Deepika Sharma, whose blessings, love, support, and consistent encouragement have enabled me to glide through my troubles with effortless ease. Special Thanks to my nephew "Bargaav Sharma," whose simplicity and childhood have brought smiles to me at times of stress. Finally, my gratitude towards the almighty for giving me determination and showing me how to be what I am today.

Devdutt Sharma

## CONTENTS

S. No.	TITLE	Page No.
I	Certificate	I
II	Declaration by the candidate	II
III	Copy right transfer certificate	III
IV	Acknowledgment	IV- V
V	Contents	VI-VII
VI	List of figure	VIII-XI
VII	List of tables	XII
VIII	List of abbreviations	XIII
IX	Preface	XIV-XV
X	Abstract	XVI- XVIII
<b>1</b>	<b>Introduction to Food Toxicants</b>	<b>1-14</b>
1.1	Food Toxicity	1-6
1.2	Monosodium glutamate and its adverse effect	6-9
1.3	Objective of the Thesis	9-10
1.4	Contribution of the Thesis	11-13
1.5	Structure of the Thesis	13-14
<b>2</b>	<b>Analytical Chemistry of Glutamate: A Literature Review</b>	<b>15-32</b>
2.1	Introduction	15-18
2.2	Non-enzymatic methods for MSG determination	18-22
2.3	Enzymatic methods for MSG determination	22-31
2.4	Antibodies-based methods for MSG determination	31-32

2.5	Miscellaneous methods	32
3	<b>Synthesis of Nanomaterials for Immunosensor Platforms</b>	<b>33-51</b>
3.1	Introduction	33-34
3.2	Synthesis of Gold-Chitosan Nanocomposites (CS-GNP)	35-40
3.3	In-situ reduction dual-metallic conjugate through polymer linkage	40-48
3.4	Synthesis of GNP through chemical route	48-51
4	<b>Preparation of Immunosensor Platforms</b>	<b>52-75</b>
4.1	Introduction	52-56
4.2	Electrochemical synthesis	56-59
4.3	Synthesis of PANI-TiO <sub>2</sub> through electrochemical polymerization	59-67
4.4	Synthesis of PANI-GNP through electrochemical polymerization	67-75
5	<b>Electrochemical Detection of MSG</b>	<b>76-109</b>
5.1	Introduction	76-78
5.2	Materials & Instrumentation	78
5.3	Electrochemical detection of MSG by GNP-chitosan nanocomposite.	79-88
5.4	Electrochemical detections of MSG by LB film of PANI-TiO <sub>2</sub>	89-100
5.5	Electrochemical detection of MSG by LB film of PANI- GNP	100-109
6	<b>Conclusions and Future Scope</b>	<b>110-113</b>
6.1	Conclusion	110-112
6.2	Future Scope	113
	<b>Reference</b>	<b>114-128</b>
	<b>List of publications</b>	<b>129</b>

## LIST OF FIGURE

<b>Figure No.</b>	<b>Figure Caption</b>	<b>Page No.</b>
Figure 1.1	Types of physical toxin	3
Figure 1.2	Types of a biological toxin	4
Figure 3.1	UV-vis spectra of CS-GNP colloidal suspension at various time (T) points (A) start of the reduction T = 0 h, (B) T = 2 h, (C) T = 4 h, (D) T = 5 h, (E) T = 6 h and (F) T = 7 h during in-situ reduction of 0.4 mM gold chloride at various concentration (C1 = 3g wt./v., C2 = 2g wt./v., C3 = 1g wt./v. and C4 = 0.5g wt./v) of chitosan.	36
Figure 3.2	UV-vis spectrum of CS-GNP gel solution.	37
Figure 3.3	FTIR spectra of CS and CS-GNP gel solution.	38
Figure 3.4	(A) XRD pattern of CS and CS-GNP film, and (B) TEM image of CS-GNP.	39
Figure 3.5	(A) Schematic representation of GNP synthesized from AuCl <sub>3</sub> /CS, (B) Schematic representation of GNP, (C) Schematic representation of DMC nanoparticles.	40
Figure 3.6	(A) Particle size distribution bar graph for GNP, (B) Transmission electron microscopy image of GNP, (C) Transmission electron microscopy image of DMC nanoparticles.	41
Figure 3.7	(A) Schematic representation of AgNP synthesized from AgNO <sub>3</sub> /CS, (B) Schematic representation of AgNP, (C) Schematic representation of DMC nanoparticles.	42
Figure 3.8	(A) Particle size distribution bar graph for AgNP, (B) Transmission electron microscopy image of AgNP, (C) Transmission electron microscopy image of DMC nanoparticles.	43
Figure 3.9	UV-vis spectra of a) gold nanoparticles, b) silver nanoparticles, c) CS-GNP-AgNP, and d) CS-AgNP-GNP.	44
Figure 3.10	XRD pattern of a) gold nanoparticles, b) silver nanoparticles, c) CS-GNP-AgNP, and d) CS-AgNP-GNP.	45
Figure 3.11	Cyclic voltammogram of a) gold nanoparticles, b) silver nanoparticles, c) CS-GNP-AgNP, and d) CS-AgNP-GNP.	47
Figure 3.12	(A) UV-vis spectrum GNP at 535 nm and optical image, (B) high-resolution TEM image of GNP.	48
Figure 3.13	(A) GNP colloidal dispersion TEM image of GNP and (B) size distribution curve.	49
Figure 3.14	(A) XRD patterns of GNP and (B) XPS Spectrum of GNP.	50
Figure 4.1	(A) UV-vis spectrum PANI at 290 nm and optical image PANI colloid disperses (B) TEM image of PANI.	56

Figure 4.2	XRD pattern of PANI.	57
Figure 4.3	(A) UV-vis spectrum of TiO <sub>2</sub> . (B) XRD pattern of TiO <sub>2</sub>	58
Figure 4.4	(A) Schematic representation of electrochemical polymerization of aniline and TiO <sub>2</sub> . (B) Diagrammatic illustration of PANI-TiO <sub>2</sub> nanocomposites.	59
Figure 4.5	CV response of electrochemical polymerizing PANI-TiO <sub>2</sub> for successive 21 cycles.	60
Figure 4.6	(A) TEM image of PANI-TiO <sub>2</sub> , (B) High-resolution TEM images showing lattice pattern of TiO <sub>2</sub> , (C) Energy dispersive X-ray analysis of PANI-TiO <sub>2</sub> nanocomposites showing the relative atomic proportion of different elements present in nanocomposites, (D) bar graph of TiO <sub>2</sub> nanoparticle size distribution in PANI-TiO <sub>2</sub> .	61
Figure 4.7	UV-vis spectra of (a) TiO <sub>2</sub> , (b) PANI and (c) PANI-TiO <sub>2</sub> .	62
Figure 4.8	Schematic illustration of L-B film deposition of PANI-TiO <sub>2</sub> .	63
Figure 4.9	Surface pressure - area (p-A) curve during optimizing of LB film deposition conditions where (a) PANI and (b) PANI-TiO <sub>2</sub> ; inset images show UV-vis spectra of (a) PANI and (b) PANI-TiO <sub>2</sub> along with optical images of their suspension in a solvent.	64
Figure 4.10	SEM image of PANI-TiO <sub>2</sub> LB film.	65
Figure 4.11	XRD spectrum of (a) TiO <sub>2</sub> , (b) PANI, and (c) PANI-TiO <sub>2</sub> .	66
Figure 4.12	Wide scan X-ray photoelectron spectra of TiO <sub>2</sub> and PANI-TiO <sub>2</sub> film surface.	67
Figure 4.13	(A) UV-vis spectrum of GNP colloidal suspension and TEM image of GNP, (B) Size distribution curve of GNP in TEM image with Image J software. (C) TEM image of single GNP.	68
Figure 4.14	XRD spectrum of GNP film on a glass substrate.	69
Figure 4.15	Electrochemical polymerization of aniline monomer in GNP colloidal suspension and CV response during electrochemical polymerization for 35 cycles.	70
Figure 4.16	Energy-dispersive X-ray analysis of PANI-GNP film surface showing the relative atomic proportion of different elements present in the LB film (inset image is high-resolution TEM of PANI-GNP).	71
Figure 4.17	XRD pattern of PANI-GNP on a glass substrate.	72
Figure 4.18	Schematic diagram of LB film deposition process.	73
Figure 4.19	Surface pressure – area (p-A) curve during optimizing of LB film deposition of PANI-GNP.	74

Figure 4.20	High-resolution Au4f X-ray photoelectron spectra of gold in (A) PANI-GNP film surface, (B) GNP film surface, and (C) C1s X-ray photoelectron spectra of carbon PANI-GNP nanocomposite film surface.	75
Figure 5.1	Schematic diagram for fabrication of working electrode platforms.	80
Figure 5.2	(A) CV and (B) DPV of different working electrodes. Glassy carbon electrode (GCE), chitosan (CS), chitosan-gold nanoparticles (CS-GNP), Rabbit anti-glutamate antibodies functionalized chitosan – gold nanoparticles (CS-GNP-AB).	81
Figure 5.3	(A) CV and (B) DPV response of CS-GNP-AB working electrode at various pH levels.	82
Figure 5.4	(A) CV response of CS-GNP-AB working electrode with different concentrations of MSG. Relative change in (B) oxidation and reduction peak potential, (C) Anodic peak current, and (D) cathodic peak current with MSG concentrations. The result was obtained for n= 4 substrates with an average error of 8% to 13%.	83
Figure 5.5	(A) DPV response of CS-GNP-AB working electrode with different concentrations of MSG. (B) Relative change in % peak current with MSG concentrations. The result was obtained for n= 4 substrates with an average error of 8% to 13%.	84
Figure 5.6	Nyquist plots at various MSG concentrations (from 1 nM to 500 nM) in electrolytes obtained from antibodies immobilized working electrode (biosensors WE) for the impedance obtained between 1 MHz and 0.1 Hz frequency variation.	86
Figure 5.7	(A) DPV response of biosensor WE (antibody immobilized CS-GNP coated GCE) and 100 nM of MSG added to the electrolyte (MSG in EL), and 100 nM of MSG added to tomato sauce (MSG in RS). (B) Bar diagram representing a relative change in peak current in response to MSG in electrolyte and real sample.	87
Figure 5.8	Schematic figure for biosensor construction.	89
Figure 5.9	(A) CV and (B) DPV of different types of working electrodes, (a) ITO electrode, (b) PANI-TiO <sub>2</sub> LB film working electrode, (c) Rabbit anti-glutamate antibodies immobilized PANI-TiO <sub>2</sub> LB film working electrode, and (d) BSA passivated rabbit anti-glutamate antibody immobilized PANI-TiO <sub>2</sub> LB film working electrode.	90
Figure 5.10	(A) CV and (B) DPV of PANI-TiO <sub>2</sub> immunosensor at various pH in acidic range and (C) CV and (D) DPV of PANI-TiO <sub>2</sub> immunosensor at different pH in basic range.	92
Figure 5.11	(A) CV response of PANI-TiO <sub>2</sub> immunosensor working electrode with different concentrations of MSG, (B) Relative change in peak potential with MSG concentrations, (C) Relative change in peak current with MSG concentrations, (D) DPV response of CS-GNP-IgG working electrode with different concentrations of MSG. (E) Relative change in % peak current with MSG concentrations varying in nM	95

	concentration, and (F) Relative change in % peak current with MSG concentrations varying in $\mu\text{M}$ concentration.	
Figure 5.12	(A) DPV response of PANI-TiO <sub>2</sub> immunosensor working electrode without and with tomato sauce at different concentrations of MSG, (B) Immunosensor response for quantification of MSG concentrations where MSG (EL) represents MSG in standard electrolyte and MSG (RS) represents MSG in tomato sauce.	97
Figure 5.13	(A) CV response of immunosensor with different analytes, (CV response of black- immunosensors, green-with MSG and red-with different analytes) and (B) Relative change in peak current of CV response while different analytes added into the electrolyte, (a) ascorbic acid, (b) arginine (c) aspartic acid (d) cysteine and (e) MSG.	99
Figure 5.14	(A) Schematic representation of electrochemical Immunosensor development.	100
Figure 5.15	(A) CV and (B) DPV of different types of working electrodes. (a) ITO electrode, (b) PANI-GNP LB film working electrode, (c) Rabbit anti-glutamate antibodies immobilized PANI-GNP LB film working electrode, and (d) BSA passivated rabbit anti-glutamate antibody immobilized PANI-GNP LB film working electrode.	102
Figure 5.16	(A) DPV of PANI-GNP immunosensor at different pH ranges.	103
Figure 5.17	(A) CV response of PANI-GNP immunosensor working electrode with different concentrations of MSG, (B) Relative change in peak potential with MSG concentrations, (C) Relative change in cathodic peak current with MSG concentrations, and (D) Relative change in anodic peak current with MSG concentrations.	105
Figure 5.18	(A) DPV response of PANI-GNP immunosensor with different concentrations of MSG in the electrolyte, (B) Relative change in % peak current with MSG concentrations in the electrolyte, (C) DPV response of PANI-GNP immunosensor with different concentrations of MSG in the real sample and (D) Relative change in % peak current with MSG concentrations in the real sample.	107
Figure 5.19	(A) DPV response of PANI-GNP immunosensor with different analytes (a) 500 $\mu\text{M}$ MSG, (b) 500 $\mu\text{M}$ Arginine, (c) 500 $\mu\text{M}$ Aspartic acid, (d) 500 $\mu\text{M}$ Cysteine, (e) without MSG. (B) Relative change in peak current with immunosensor.	108
Figure 6.1	Fabrication of three electrode systems (strip on right side of the voltage converting black color device) by physical patterning for the possible use of different platforms developed in this study as point-of-care devices.	111
Figure 6.2	(A) Schematic diagram of proposed point-of-care diagnostic system. (B) Image of electrode fabricated for a point-of-care diagnostic system with the use of reduced graphene oxide conducting ink. (C) Showing different combinations of the conducting ink printed pattern with reduced graphene oxide conducting ink.	112

## LIST OF TABLES

<b>Table No.</b>	<b>Table Caption</b>	<b>Page No.</b>
Table 1.1	Toxicity of food additives	6
Table 1.2	MSG is natural foods	7
Table 1.3	MSG is seafood, poultry, and meat foods	8
Table 2.1	Chronology of US FDA, concerns about MSG.	17
Table 5.1	Relative comparison of different types of biosensors for the detection of MSG	77

## LIST OF ABBREVIATIONS

S. No.	Abbreviations	
1	MSG	Monosodium glutamate
2	HPLC	High-Performance Liquid Chromatography
3	GC	Gas Chromatography
4	CE	Capillary Electrophoresis
5	$I_{pc}$	Cathodic peak currents
6	$I_{pa}$	Anodic peak currents
7	$E_{p,c}$	Cathodic peak potential
8	$E_{p,a}$	Anodic peak potential
9	ITO	Indium Tin Oxide
10	PANI	Polyaniline
11	BSA	Bovine Serum Albumin
12	LB	Langmuir-Blodgett
13	CV	Cyclic voltammetry
14	DPV	Differential pulse voltammetry
15	EDC	N-(3 dimethylamino propyl)-N'-ethyl carbodiimide hydrochloride
16	NHS	N-hydroxysuccinimide
17	NMP	N-methyl-2-Pyrrolidone
18	EIS	Electrochemical impedance spectroscopy

## PREFACE

This thesis is submitted for the degree of doctor of philosophy at Indian Institute of Technology (Banaras Hindu University), Varanasi. The research described herein was conducted under the supervision of Dr. Marshal in the school of biomedical engineering, Indian Institute of Technology (Banaras Hindu University), Varanasi, between July 2018 to July 2022.

This work is the best of my knowledge, original except where acknowledgment and reference are made to previous work. Neither this nor a substantially similar thesis has been or is being submitted for any other degree, diploma, or other qualification at any other university.

In 1908, Professor Kikunae Ikeda produced the first monosodium glutamate. Monosodium glutamate is frequently used in food processing units, restaurants, and packed food industry as a taste enhancer. It was produced commercially under the trade name Ajinomoto. Indian food Industries also use MSG, and it's consumption is estimated at 10510 tons per year. Food having MSG is labeled as code E-621. Glutamic acid has two optical isomer L- glutamic acid and D- glutamic acid. Only L- glutamic acid is used as a flavor enhancer in food. The taste of MSG is known as the UMAMI taste. Glutamate also plays a vital and many essential roles in metabolic processes. It is also used to transfer energy transport of amino acid across the cell membrane and remove ammonia by the urea cycle. Glutamate also acts as a neurotransmitter and its brain metabolic rate.

But in 1990 in the USA, a particular population reported headaches, nausea, and vomiting after eating food having MSG. These syndrome collectively is known as Chinese restaurant syndrome.

In 1995, FDA declared MSG as generally safe and decided its maximum permissible limit. India's Prevention of Food Adulteration Act defined the permissible MSG content in food as 1%.

Most recently, a controversy flared up when the food safety and drug administration, Utter Pradesh, found high level of MSG in Maggi noodles. The government issued a notice to Nastle to recall this product from the market. As per the FSSAI guidelines, MSG is not permitted in pasta and noodles. So, food industries should need sample, fast, highly selective, highly sensitive, efficient, and cost-effective methods of MSG quantification. The monitoring of glutamate is also essential for fermentation control during its production

The present thesis's objective was to detect monosodium glutamate's electrochemical detection by the self-assemble thin film of the polymer-metal nanocomposite. This thesis will be beneficial for the researcher/ academics / industrial working in the area of electrochemical quantification of monosodium glutamate biosensor

Part of this thesis published in the following publication

- **Devdutt Sharma**, Rashmita Devi, Juhi Jaiswal, Hemant Sankar Dutta, Raju Khan, and Marshal Dhayal. "A Highly Sensitive Immunosensor Based on In Situ Reduced Gold-Chitosan Nanocomposite for Detection of Monosodium L-glutamate." *Journal of Biosystems Engineering* (2022): 1-11. doi.org/10.1007/s42853-022-00127-z.
- **Devdutt Sharma**, Hemant Sankar Dutta, and Marshal Dhayal. "Langmuir-Blodgett Monolayer of Electrochemically Synthesized PANI-TiO<sub>2</sub> Nanocomposites for MSG Biosensor. " *Journal of Applied Surface Science Advances*. doi.org/10.1016/j.apsadv.2022.100264

Part of this thesis communicated in the following publication

- **Devdutt Sharma**, Hemant Sankar Dutta, and Marshal Dhayal. "Biosensor Platform of Hydrophobic Nanoassemblies of Positively Charged Polyaniline-Gold on Piranha Treated ITO by Langmuir-Blodgett Film for Electrochemical Sensing of MSG" with Sensors and Actuators B.
- **Devdutt Sharma**, Marshal Dhayal. "Dual metal conjugate through polymer linkage to enhance conductivity and catalytic degradation of Evans Blue under visible light for environmental remediation". With Colloid and Polymer Science.

## ABSTRACT

This work focused on developing metal nanomaterials with hydrophobic characteristics to deposit through the Langmuir-Blodgett (LB) film process. It is expected that a monolayer of metallic nanomaterials with enhanced conductivity could provide a better choice for effective transportation of charge and improved biomolecule adsorption capabilities compared to other methods and materials used for developing immunosensor platforms. An immunosensor based on the monoclonal anti-glutamate antibodies immobilization onto a thin film of new nanocomposites of polymer-metallic nanoparticles, conductive polymer-metal oxide nanoparticles, and conductive polymer-metallic nanoparticles through a self-assembly process developed. New platforms developed in this thesis concurrently manage functional groups' availability for antibody immobilization with enhanced electrical conductivity. An antibodies-based immunosensor is ideal for industrial applications since it allows for detecting MSG at concentrations ranging from nanomolar to micromolar on a single platform. A hypothesis for low concentration detection is proposed by considering the following facts;

In-situ reduced chitosan gold nanoparticles matrix provides both higher sensitivity and extended limit of the detection range of MSG. It is expected that impregnation of the in-situ reduced gold nanoparticles in the chitosan network provides better charge transportation and enhanced selective functionalization capability and biocompatibility. The proposed in-situ reduced gold nanoparticles may have better chemical coordination and homogeneous distribution in the chitosan network. Thus, this reduction process has an advantage over the methods that adopt the physical mixing of nanoparticles with polymeric materials. An enhancement of four-fold in current has been achieved by incorporating GNP in chitosan. The formulation also has the advantage of stable and adhesive coatings on working electrodes to develop a platform based on monoclonal anti-glutamate antibodies immobilization, Coating of these nanomaterials allowed to achieve the highest detection

sensitivity with the lowest detection limit of 0.1 nM. Electrochemical characteristics of chitosan-gold nanoparticles were studied by measuring relative change in redox current compared to standard working electrodes. Antibodies' interaction with the CS-GNP platform was confirmed through a reduction in electrochemical current.

The second method uses the titanium dioxide ( $\text{TiO}_2$ ) nanoparticles in the PANI matrix and optimizes conditions for preparing LB films of the polyaniline- $\text{TiO}_2$  nanocomposite. A unique strategy was adopted in which electrochemical polymerization of aniline in the presence of  $\text{TiO}_2$  nanoparticles was performed on ITO substrate, dissolving it in a solution of NMP and isopropanol, and LB film deposition of contamination-free subphase of PANI- $\text{TiO}_2$ . Thus, the work achieved a higher degree of polymerization through the electrochemical process and subsequently used this polymerized material to make LB film. The antibodies immobilized electrodes were successively used to quantify MSG ranging from 1 nM to 500  $\mu\text{M}$  in the standard electrolyte. A linear relationship was obtained between the current change and the MSG concentration.

In the third method, the chemical synthesized of surfactant-free stable ultra-small gold nanoparticles (< 10 nm diameter) in the PANI matrix were used. Electrochemical polymerization of aniline monomers with these gold nanoparticles was performed on ITO substrate. This unique method enabled the synthesis of polyaniline-GNP nanocomposite with hydrophobic nature. Further, this PANI-GNP nanocomposite was dissolved in a solution of NMP and isopropanol, and the conditions were optimized for preparing LB films of the polyaniline-GNP nanocomposite. The developed thin film shows a very high conductivity with improved capability for the adsorption of biomolecules. The developed electrochemical biosensor shows stability over a wide range of pH values. Antibodies immobilized immunosensor were sequentially used to quantify MSG ranging from 1 nM to 10 mM in the standard electrolyte and 1  $\mu\text{M}$  to 1 mM in tomato sauce. A linear relationship was obtained between the current change and the MSG concentration.

The electrochemical properties of all the immunosensors mentioned above were investigated by measuring the relative change in redox current compared to standard working electrodes. To improve measurement sensitivity, monoclonal anti-glutamate antibodies were bound to the amine-functionalized spots on the working electrode using the carbodiimide coupling technique. Since monoclonal anti-glutamate antibodies were used due to their ability to bind the uniquely designed substrate and arrange reactive groups in a manner that promotes a specific reaction transition state, they give these antibodies their selectivity. Monoclonal anti-glutamate antibodies show stereoselective properties ( e.g., the monoclonal anti-glutamate antibodies used in work reported in this thesis are specific for the L-isomer of glutamate). The developed immunosensors can quantify the concentration of MSG in the nano-molar range with higher stability and reproducibility.

This thesis work will be beneficial for the researcher/ academics / industrial working in the area of electrochemical quantification of monosodium glutamate biosensor